


NANO EXPRESS

Open Access



Reducing and Uniforming the Co_3O_4 Particle Size by Sulfonated Graphenel Polymers for Electrochemical Applications

Xin Zhang^{1,2†}, Xubo Liu^{2,3†}, Sha Zeng², Jianhui Fang¹, Chuanling Men³, Xiaohua Zhang^{2*}  and Qingwen Li²

Abstract

A novel two-dimensional (2D) nanomaterial, namely sulfonated graphenel polymer (SGP), is used to tune the hydrothermal growth of Co_3O_4 nanoparticles. SGP provides abundant nucleation sites to grow Co_3O_4 nanoparticles and effectively reduces the particle size and dimension. As a result, with considering the improved size uniformity of Co_3O_4 and the tight wrapping of SGP around Co_3O_4 as well, the Co_3O_4 /SGP hybrid electrode exhibits a high specific electrochemical capacitance of 234.28 F/g at a current density of 0.2 A/g, 237% higher than that of the pure Co_3O_4 electrode. By using the hybrid as the anode of an all-solid-state asymmetric supercapacitor, the capacitance can be well maintained up to 93% after 5000 cycles even at 2 A/g.

Keywords: Sulfonated graphenel polymer, Cobalt oxide, Hydrothermal growth, Electrochemical

Background

Owing to their high power density, cycle efficiency, and charge/discharge rate, supercapacitors are considered as promising candidates in energy storage applications [1–4]. There are two types of supercapacitors according to their different charge storage mechanisms, namely electric double-layer capacitors and pseudocapacitors [5]. Electric double-layer capacitor stores energy by interfacial charge separation between its electrode and the electrolyte, while pseudocapacitor realizes the charge storage mainly through the pseudo-faradaic reactions [6]. The former usually has a high performance in power density and the latter is preferred to approach a high energy density. To further improve the energy density, and specific capacitance as well, transition metal oxides, e.g., Co_3O_4 , MnO_2 , NiO , and RuO_2 , are widely used in the electrodes of supercapacitors [7–10]. In general, these transition metal oxides should be small sized (towards a high surface area), uniformly distributed, and highly crystallized. Obviously, the synthesis and assembly of these particles are of great

importance for the electrode performances, especially for the energy density and rate of capacitance [11].

Hydrothermal process is a common way to grow metal oxide nanoparticles [12]. To control the particle size, crystallinity, and particle morphology, the introduction of nanoplatelets has been proved as an efficient strategy [13–16]. For example, graphene oxide (GO) has exhibited exciting effects as it can provide rich active sites to anchor the nanoparticles, prevent their agglomeration, and avoid the overgrowth. This is owing to its two-dimensional (2D) nanostructure, abundant functional groups, and high specific surface area [15, 16]. As a result, needle-like Co_3O_4 nanoparticles with a size of 10–50 nm or cross-like NiO nanoflakes with a thickness of ~15 nm were grown on GO [17, 18].

In this study, we report a facile way to precisely control the size and distribution of Co_3O_4 nanoparticles on a new type of 2D nanostructure, namely sulfonated graphenel polymer (SGP), by a hydrothermal process. On the one hand, the abundant sulfonic acid groups of SGP make it superhydrophilic and thus allow efficient adsorption of metal cations [19]. Therefore, there exist rich anchor sites for the growth of Co_3O_4 . On the other hand, the polymeric characteristics of SGP [20], due to its irregular or branched 2D planar structure, result in high flexibility and thus tight wrapping of SGP around

*Correspondence: zhangxhcm@gmail.com

[†]Equal contributors

²Suzhou Institute of Nano-Tech and Nano-Bionics, Chinese Academy of Sciences, Suzhou 215123, China

Full list of author information is available at the end of the article

the Co_3O_4 nanoparticles. The Co_3O_4 /SGP hybrid electrode can exhibit a high specific capacitance of 234.28 F/g at a current density of 0.2 A/g, which was 237% higher than that of the pure Co_3O_4 electrode (69.5 F/g). By using the Co_3O_4 /SGP electrode as the anode of an all-solid-state asymmetric supercapacitor, a high reversibility was achieved due to the reduced and uniformized particle size and intimate contact between the Co_3O_4 /SGP hybrid with the conducting fillers. After 5000 cycles even at 2 A/g, the capacitance was still maintained up to 93%. As compared to GO, this study demonstrates an interesting potential of SGP in the electrochemical applications.

Methods

Materials Synthesis

The SGP nanostructures in this study were purchased from Suzhou Graphene-Tech Co., Ltd. and were used as received. They were synthesized by a “bottom-up” strategy [20] where the reaction between polyethylene and fluorosulfuric acid were conducted [21]. After the fluorosulfuric acid (concentration over 99%) was heated up to 70–80 °C, polyethylene was added to trigger the reaction. The polymer-to-acid weight ratio was within 1:10 to 1:15. After 10 min, the reaction product was separated by water to obtain SGP dispersions, which can be further dried to obtain SGP powders. In this study, the as-received SGP powder was dispersed in deionized water to obtain a 0.1 wt% SGP solution.

For the Co_3O_4 growth, 1 mmol cobalt acetate ($\text{Co}(\text{CH}_3\text{COO})_2 \cdot 4\text{H}_2\text{O}$ or $\text{Co}(\text{OAc})_2 \cdot 4\text{H}_2\text{O}$) was dissolved in 45 ml water, mixed with 5 ml 0.2 M aqueous NaOH solution, and then stirred for 5 min. The solution was transferred into Teflon-lined stainless steel autoclave and then maintained at 120 °C for 12 h to start the Co_3O_4 growth. After the reaction, the solution was cooled naturally to room temperature and then dried at 80 °C for 12 h. The SGP-assisted Co_3O_4 growth had the same treatment sequence, except additional 5 ml 0.1 wt% SGP solution was added into the mixture (the total volume was still 50 ml just by dissolving the same amount of $\text{Co}(\text{OAc})_2$ into 40 ml water). In order to study the effect of the solution basicity, the similar Co_3O_4 growth was also performed in an NH_3 solution. Here, NaOH was replaced by 9 ml $\text{NH}_3 \cdot \text{H}_2\text{O}$ without tuning the amounts for the other compounds (the total volume was also fixed to 50 ml). By using these two different growths, Co_3O_4 /SGP hybrid or composite powders were obtained.

Electrode and Supercapacitor Preparations

Five milligrams of Co_3O_4 or Co_3O_4 /SGP powder was added to ethanol, and then blended with 0.5 mg multiwall carbon nanotubes (MWCNTs) which acted as the conductive agent. The mixture was dried at 80 °C for 1 h and then packaged with a 1-cm² Ni foam. The foam was dried

at 110 °C for 12 h under a vacuum oven, and then pressed under 10 MPa to form a working electrode.

To better evaluate the electrochemical performance, a supercapacitor was made by assembling the Co_3O_4 electrode as the anode, active carbon as the cathode, and poly(vinyl alcohol) (PVA)/KOH as the separator. The gravimetric specific capacitance for the whole supercapacitor cell was calculated from the galvanostatic charge/discharge (GCD) curve by considering the total mass of Co_3O_4 , SGP, and CNT, namely, the mass increase of the Ni foam.

Electrochemical Measurements

The electrochemical performance of electrode was measured using a three-electrode test in a 6 M KOH solution at room temperature, with a Chenhua CHI-660C electrochemical workstation. A platinum mesh and a saturated Hg/HgO electrode were used as the counter and reference electrodes, respectively. Cyclic voltammetry (CV), GCD, and electrochemical impedance spectroscopy (EIS) were carried out using conventional three-electrode configurations at a potential range of 0–0.4 V or in a frequency range of 100 kHz to 0.01 Hz. The specific capacitance (C_s) was calculated from the GCD data by $C_s = It/m\Delta V$, where I is the applied current, t the time for the discharge process, m the mass of the active material, and ΔV the potential range [22, 23].

Characterizations

The Co_3O_4 structure was characterized by a Quanta 400 FEG field emission scanning electron microscope (SEM) equipped with an Apollo 40 SDD energy-dispersive X-ray spectroscopy (EDS) for element determination and by an FEI Tecnai G2 F20 S-Twin transmission electron microscope (TEM). Lateral dimensions and thickness of SGP nanosheets were characterized using tapping-mode atomic force microscope (AFM; Bruker Instruments Dimension Icon) with a silicon-tip cantilever (40 N/m). The Fourier transform infrared spectroscopy (FTIR) (500–4000 cm^{−1}) was measured using a Nicolet 6700 FTIR spectrometer. The surface area was measured by the Brunauer-Emmett-Teller (BET) method with a Micromeritics ASAP 2010 sorptometer. The crystal structure was examined by a Bruker AXS D8 Advance X-ray diffraction (XRD) system.

Results and Discussion

Structure of SGP

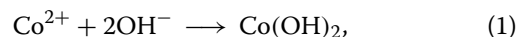
As a new type of graphenel polymer [20], SGP possessed common features such as large specific surface area, good physical and chemical stability, flexibility, and adhesiveness. So far, the first study on SGP was the application in the electrolyte separator for all-solid-state supercapacitors where SGP nanosheets were self-assembled into a

highly porous film with the aid of intermolecular adhesion by PVA [24]. To show the nanostructure of SGP, SEM and AFM were performed, see Fig. 1a, b. SGP showed a 2D planar structure while the 2D plane was quite irregular as porous and branched structures were widely observed (Fig. 1a). This was a result of the bottom-up synthesis procedure [20]. The SGP nanosheets were about 4–5 layered according to the thickness of ~ 4 nm (Fig. 1b). The Raman spectrum showed two peaks centered at 1585 and 1382 cm^{-1} which were typically the G- and D-peaks for the carbon sp^2 structure (Fig. 1a, inset).

Further, the sulfonic acid group ($-\text{SO}_3\text{H}$), carboxyl group ($-\text{COOH}$), and hydroxyl group ($-\text{OH}$) were detected as strong absorption peaks with FTIR, as shown in Fig. 1c. Besides the wide absorption band for $-\text{OH}$ centered around $3200\text{--}3550\text{ cm}^{-1}$, the absorption bands at 1043 and 1171 cm^{-1} were due to the SO_2 symmetric and asymmetric stretching, and the absorption between $1650\text{--}1720\text{ cm}^{-1}$ was related with $-\text{COOH}$. Based on these structural characteristics, such 2D nanostructure was named as sulfonated graphenel polymer. Furthermore, the abundant sulfonic acid and carboxyl groups resulted in superhydrophilicity for SGP, as these molecules can be dispersed in water at high concentrations even up to 26 wt%. As shown in Fig. 1d, the 20 wt% SGP dispersion still showed a high fluidity while the 2 wt% GO dispersion nearly became a hydrogel.

SGP-assisted Co_3O_4 Growth

Co_3O_4 nanoparticles were fabricated with a hydrothermal approach by using $\text{Co}(\text{OAc})_2$ as the source material. Under a basic environment (0.02 M NaOH solution), $\text{Co}(\text{OAc})_2$ converted into Co_3O_4 after several hours, according to the following reactions [14, 25, 26]:



SGP can strongly influence the Co_3O_4 growth. Without SGP, the particle size was quite diverse, ranging from 50 to 200 nm (Fig. 2a and b). The large-sized Co_3O_4 nanoparticles were the agglomeration of small-sized particles due to the lack of nucleation sites [27]. On the contrary, the presence of SGP can provide sufficiently more nucleation sites to anchor $\text{Co}(\text{OH})_2$ clusters for the direct Co_3O_4 growth on SGP, owing to the abundant $-\text{OH}$ groups [28]. These groups can also reduce the divergence in growth rate at different sites and hinder the overgrowth due to the space limit. As a result, the SGP-assisted growth showed an improved uniformity in particle size, see Fig. 2d, e. In general, even after a 12-h growth, the Co_3O_4 particles on SGP were still about 20–30 nm in diameter, while the free growth just in 3 h could cause a particle size over 100 nm.

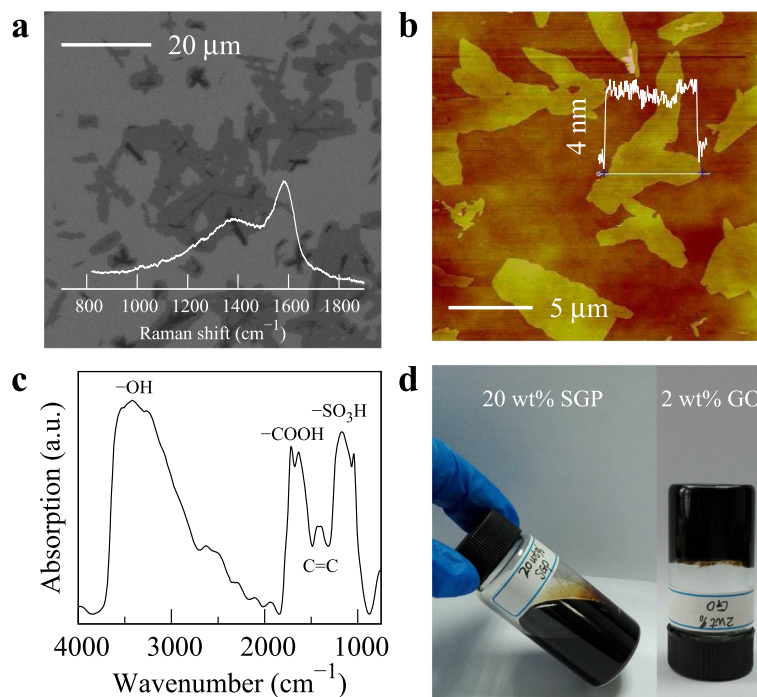


Fig. 1 **a, b** SEM and AFM images of SGP nanosheets with insets showing the Raman spectrum and film thickness. **c** FTIR spectrum shows high fractions of $-\text{SO}_3\text{H}$, $-\text{COOH}$, $\text{C}=\text{C}$, and $-\text{OH}$ groups. **d** Optical images of a 20 wt% SGP dispersion (still a liquid) and 2 wt% GO dispersion (gel like)

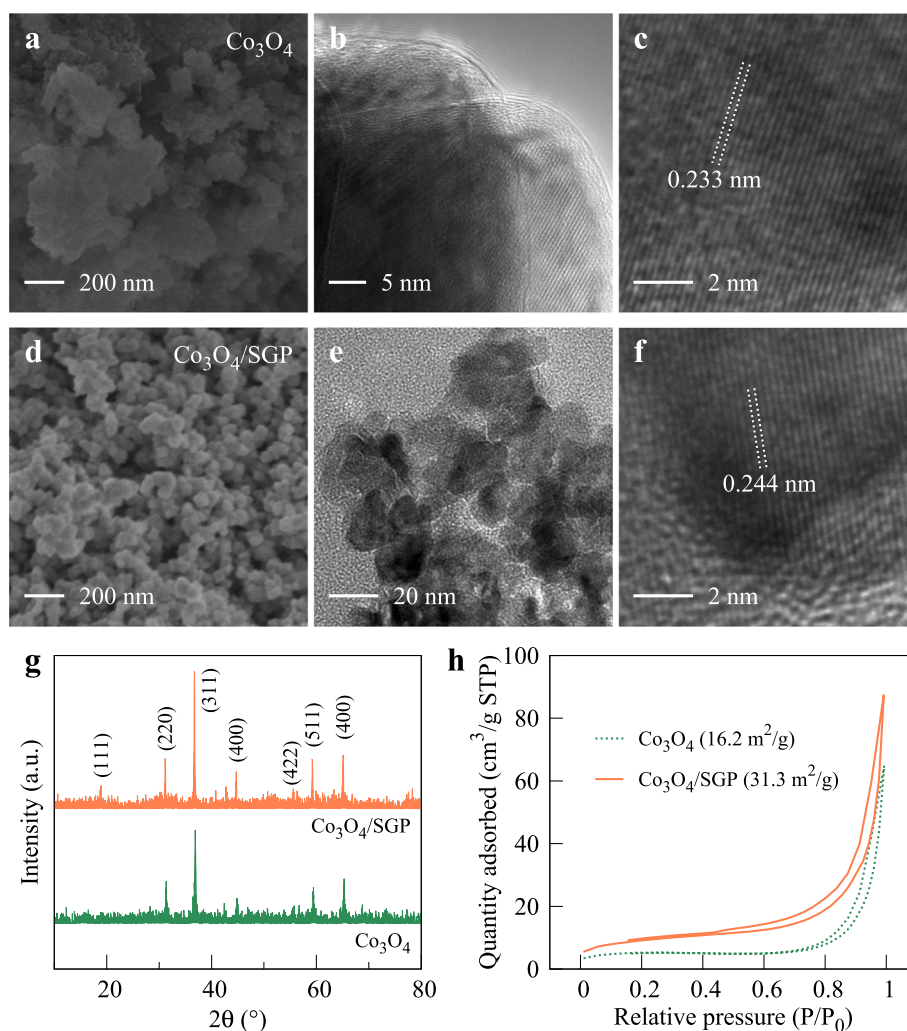


Fig. 2 **a–c** SEM and TEM images showing that the Co_3O_4 particles were 50–200 nm sized and the interplanar distance of 0.233 nm corresponded to the stacking of (311) planes. **d–f** SGP reduced the particle size down to sub-20 nm, while the similar (311) stacking was observed with an interplanar distance of 0.244 nm. **g, h** XRD patterns and N_2 adsorption-desorption isotherms for the Co_3O_4 and $\text{Co}_3\text{O}_4/\text{SGP}$ powders

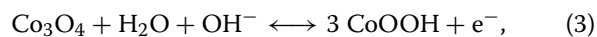
The reduced particle size did not affect the crystallinity. Figure 2c, f compares the TEM results for the free and SGP-assisted growths. Both structures showed an interplanar spacing of 0.233–0.244 nm, by averaging the length of 20 lattices, corresponding to the (311) plane of fcc Co_3O_4 . XRD measurements (Fig. 2g) also showed diffraction peaks at 18.9° , 31.1° , 36.8° , 44.7° , 55.6° , 59.3° , and 65.1° , which were assigned to (111), (220), (311), (400), (422), (511), and (440) crystal planes. For both growths, the (311) diffraction peak was the most strongest one, in agreement with the TEM characterization.

The reduced particle size increased significantly the specific surface area. Figure 2h shows a comparison of the BET surface area. The presence of SGP increased the specific surface area from 16.2 m^2/g for the free growth up to 31.3 m^2/g . The improved surface area could increase

the contact area between the electrode and electrolyte, provide more surface reaction sites, and thus benefit the electrochemical performance.

Electrode Performance

The electrochemical properties of the Co_3O_4 and $\text{Co}_3\text{O}_4/\text{SGP}$ electrodes were investigated with a three-electrode test in a 6 M KOH solution. The electrodes were prepared in a conventional way by using MWCNTs as conductive additives. 0.5 mg MWCNTs were blended with 5 mg Co_3O_4 or $\text{Co}_3\text{O}_4/\text{SGP}$ powders, and then packaged inside 1- cm^2 Ni foam. In electrochemical measurement, the potential window was 0–0.4 V against the Hg/HgO reference electrode [8, 29]. The redox reactions at the Co_3O_4 electrode can be described by the following sequences [16]:



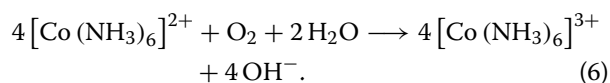
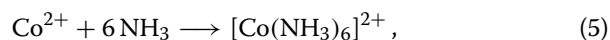
The reduced particle size and increased surface area of Co_3O_4 benefited the electrochemical properties. As compared to the free-grown Co_3O_4 , the Co_3O_4 /SGP hybrid electrode exhibited enhanced CV and GCD performances (Fig. 3a, b). The specific capacitance of the Co_3O_4 /SGP hybrid electrode was up to 100.3 F/g at a current density of 0.2 A/g, which was 144% higher than that of the Co_3O_4

electrode (69.5 F/g at 0.2 A/g). The charge/discharge time at 2 A/g also increased from 19 to 28 s after the SGP-assisted growth. Notice that both SGP and CNT did not contribute to the electrochemical activity by themselves as they are much less active than Co_3O_4 . In Fig. 3a, the CV curves for SGP and CNT are also provided for comparison, where these carbon materials were packed into Ni foams at a mass of 0.5 mg.

To better understand the improved performance of the Co_3O_4 /SGP electrode, EIS was employed to investigate the reaction kinetics. The Nyquist plots of different samples, which were characterized by a semicircle in the high-frequency region and a straight line in the low-frequency region, are shown in Fig. 3c. In general, the bigger diameter of the semicircle, the bigger charge transfer resistance between the electrode and electrolyte [30]. Obviously, the hybrid sample showed a lower charge transfer resistance, corresponding to the improved electric conductivity.

Effect of Solution Basicity

NaOH is a strong base and can induce rapid growth of Co_3O_4 , as the highly polar OH^- groups can easily coordinate with Co^{2+} . As a result, the as-produced Co_3O_4 nanoparticles were spherical in shape even under the SGP-assisted growth, see Fig. 2d–f. In order to suspend the growth rate and thus restrict the particle shape or size, a less basic solution, a 2.36 M NH_3 solution, was used to produce the Co_3O_4 /SGP hybrids. The synthetic processes were based on the relatively weak coordination between Co^{2+} and NH_3 , as described by the following reactions [31–33]:



Then, these coordinate ions decomposed at a certain temperature (usually via a hydrothermal process), and finally, Co_3O_4 nanomaterials were obtained [31].

Figure 4a shows the agglomeration morphology of Co_3O_4 nanoparticles obtained in the NH_3 solution. As compared to Fig. 2d, the particle did not have a smooth surface but looked like assemblies of low-dimensional nano-structures. TEM characterization showed that 2D Co_3O_4 nanoplatelets with lateral size of 25–30 nm were grown in the NH_3 solution (Fig. 4b). Clearly, the particle size was well controlled both in the particle size due to the presence of growth substrate of SGP and in the particle dimension due to the decreased basicity.

Nevertheless, a general structure was obtained despite the different basic solutions. By tracing from an empty place to the surface of a Co_3O_4 nanoparticle, the element counting of Co, O, and S increased simultaneously at the particle surface, see the EDS curve shown

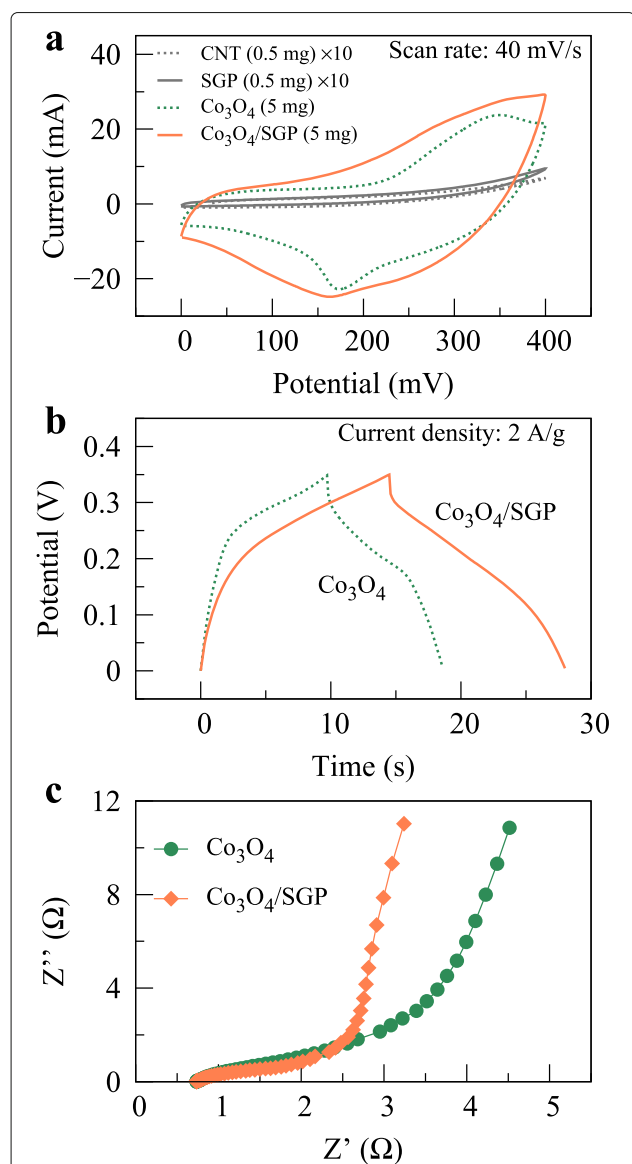


Fig. 3 **a** CV curves at a scan rate of 40 mV/s for the Co_3O_4 and Co_3O_4 /SGP hybrid electrodes. The mass of activate materials was 5 mg. For a comparison, the CV curves for SGP and CNT (mass 0.5 mg) were provided, with a magnification factor of 10. **b** GCD behaviors at a current density of 2 A/g. **c** EIS spectra measured at a frequency range of 100 kHz to 0.01 Hz

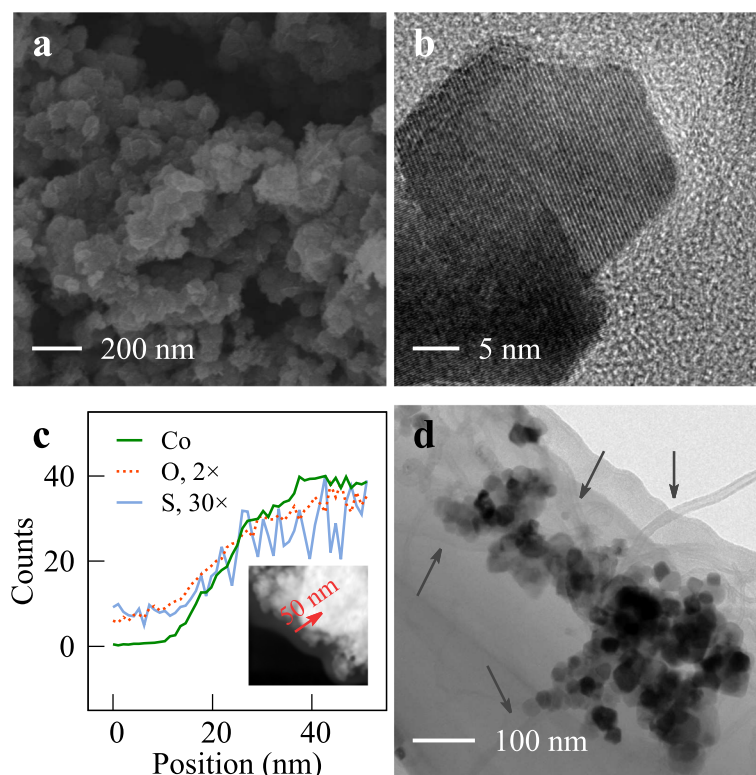


Fig. 4 **a** The Co_3O_4 /SGP nanoparticles grown in NH_3 solutions were agglomerations of 2D nanoplatelets. **b** The Co_3O_4 nanoplatelets had a lateral dimension of 25–30 nm. **c** EDS characterization showed that the Co_3O_4 nanoparticles were tightly wrapped by SGP. **d** After blending, the Co_3O_4 nanoplatelets had an intimate contact with MWCNTs, labeled by arrows

in Fig. 4c. This means that the Co_3O_4 nanoparticles were tightly wrapped by SGP, clearly due to its irregular and flexible 2D structure. Notice that, from SEM or TEM images in Figs. 2 and 4, it was difficult to observe any planar nanostructures as shown in Fig. 1. This was another important observation to show the high flexibility of SGP. Such tight wrapping can reduce the charge transfer distance from the surrounding solution to the inside of the nanoparticle, and thus is important for the electrochemical performance. Furthermore, these Co_3O_4 /SGP hybrid nanoparticles formed intimate contact with MWCNTs after the blending to prepare electrodes, see the TEM image in Fig. 4d. This also indicated that the small-sized and low-dimensional Co_3O_4 nanoplatelets could exhibit superior electrochemical performances.

Notice that, the SGP-assisted growth can be directly compared with the Co_3O_4 growth on GO [32], by using the same source material ($\text{Co}(\text{OAc})_2$) and basic solution ($\text{NH}_3 \cdot \text{H}_2\text{O}$). Due to the reduced basicity, both growths produced Co_3O_4 nanoparticles with a particle size no larger than 25 nm, attributed to the coordination between Co^{2+} and NH_3 in reducing the Co_3O_4 particle size [31, 32]. However, clear difference could

be observed at the particle dimension. The less functionalization level of GO, as compared to SGP, still causes the formation of 3D Co_3O_4 nanospheres, different from the SGP-induced dimension reduction of Co_3O_4 nanoplatelets.

The reduction in particle dimension could greatly benefit the specific surface area. Figure 5a compares the BET measurements of the Co_3O_4 nanoparticles obtained from the two solutions. Surprisingly, the dimension reduction increased the specific surface area significantly from 31.3 to 134.5 m^2/g . Based on such advantage, the electrode performance was also improved remarkably by NH_3 . Under a scan rate of 40 mV/s, the internal area of CV curve for Co_3O_4 /SGP composite grown in NH_3 was apparently larger than that of Co_3O_4 /SGP composite grown in NaOH (Fig. 5b), implying that the specific capacitance could be improved remarkably by NH_3 . The current intensity at oxidation peaks of CV increased from 25 to 30 mA at a voltage of ~ 350 mV, and the redox peak also became broader. By comparing Fig. 3a and Fig. 5b, one can find that the CV curve became more rectangular and the redox peaks became much wider, possibly due to the enhanced charge transfers from the dimension reduction. Figure 5c further shows that the charge/discharge time at 2 A/g

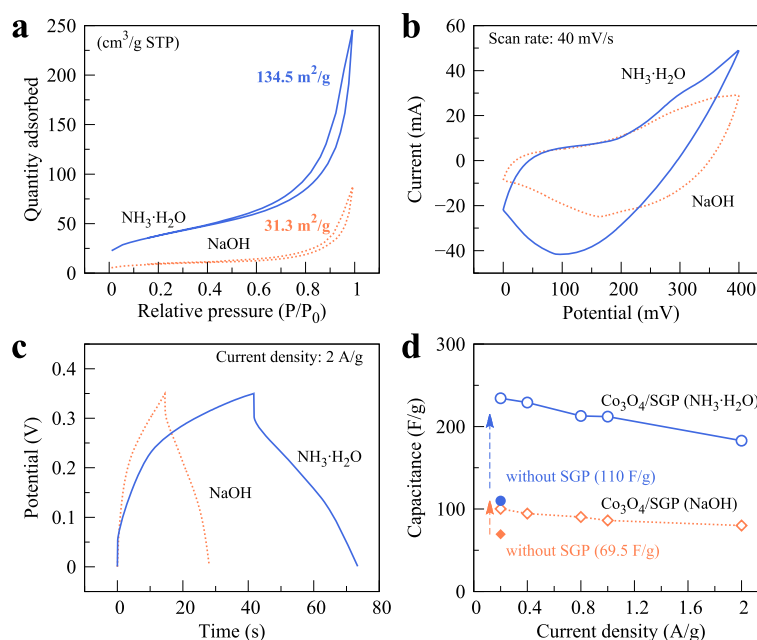


Fig. 5 **a** N_2 adsorption-desorption isotherms for the Co_3O_4 nanoparticles grown in the NaOH and NH_3 solutions. **b, c** Comparisons in CV and GCD for different Co_3O_4 growths. **d** Specific capacitances at current densities ranging from 0.2 to 2 A/g. For a comprehensive comparison, the capacitances at 0.2 A/g for the free growth in different solutions were also plotted

increased from 28 to 32 s by changing the basic environment from NaOH to NH_3 . As a result, the specific capacitance of the $\text{Co}_3\text{O}_4/\text{SGP}$ (obtained by NH_3) hybrid electrode was up to 234.28 F/g at a current density of 0.2 A/g (Fig. 5d), which was 134% higher as compared to the SGP-assisted growth in NaOH (100.3 F/g), and was 3.37 and 2.13 times those of the pure Co_3O_4 electrodes obtained from NH_3 (69.5 F/g) and NaOH (110 F/g), respectively.

Notice that, the electrode capacitance was not as high as up to about 500–1000 F/g in many recent literature [8, 12, 14, 16]. The possible reasons could be the un-intimate contact between the activate material with Ni foam, the low electrical conductivity of CNT, and the un-uniform distribution of Co_3O_4 with CNT, due to the physical blending. This was similarly reported in some other literature where the capacitance was only up to about 150–270 F/g [17, 34, 35]. Nevertheless, as all the electrodes were prepared under the same method, the present study could still show the exciting advantage of SGP in improving the deposition of metal oxides.

Application in Supercapacitors

To further investigate the $\text{Co}_3\text{O}_4/\text{SGP}$ electrode performance, the hybrid was assembled with active carbon and PVA/KOH electrolyte to an all-solid-state asymmetric supercapacitor, where the $\text{Co}_3\text{O}_4/\text{SGP}$, active carbon, and

PVA/KOH acted as the anode, cathode, and separator, respectively. The two electrodes were integrated with Ni foams for a better current collection. The gravimetric specific capacitance for the whole supercapacitor cell was calculated from the GCD curve by considering the total mass of the two electrodes.

In the supercapacitor, the $\text{Co}_3\text{O}_4/\text{SGP}$ electrode exhibited explicit redox peaks of pseudocapacitor and excellent cycle stability. With increasing the scan rate from 5 to 40 mV/s, the current intensity at oxidation peaks of CV increased correspondingly from 2.5 to 9.7 mA (Fig. 6a). The GCD curves of the $\text{Co}_3\text{O}_4/\text{SGP}$ at different current densities showed the Faradaic characteristics, in agreement with the CV curves (Fig. 6b). The specific capacitance was 84.0, 75.6, 74.5, and 57.0 F/g at current densities of 0.4, 0.8, 1, and 2 A/g, respectively, reflecting the common performance in the three-electrode system (Fig. 6c).

Furthermore, the cycle charge/discharge test was employed at a current density of 1 A/g, as shown in Fig. 6d. Owing to the small-sized Co_3O_4 and the SGP wrapping, the device demonstrated an excellent stability, remaining 93% of its initial capacitance even after 5000 charge/discharge cycles. Notice that the specific capacitance slightly grew up in the first 500 cycles. This could be a result of electrochemical activation due to the increase in contact area between the electrode and the electrolyte during the cycling [36]. As compared to the previous

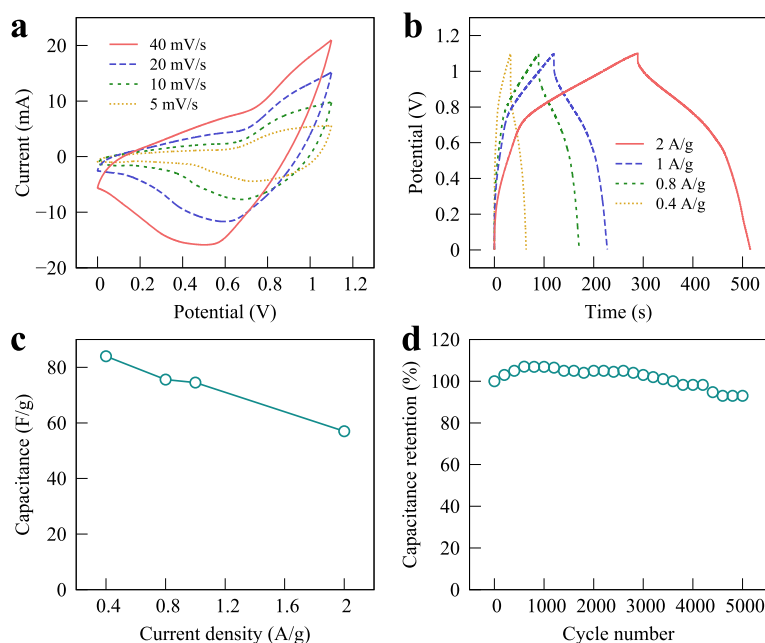


Fig. 6 **a** CV curves for an asymmetric supercapacitor with the $\text{Co}_3\text{O}_4/\text{SGP}$ acting as the anode. **b, c** GCD curves and specific capacitances at different current densities. **d** Cycling performance at a current density of 1 A/g

reports [17], where $\sim 70\%$ capacitance was maintained after 4000 cycles, the present results obviously demonstrate an exciting potential for the application in energy storage devices.

Conclusions

SGP-wrapped Co_3O_4 nanoparticles with uniform particle size were synthesized with a hydrothermal process. As a result of the reduced particle size and wrapping assembly, the $\text{Co}_3\text{O}_4/\text{SGP}$ hybrid exhibited superior electrochemical performance due to the increased BET surface area and the improved interfacial electrical conductivity. By tuning the basic solution from NaOH to NH_3 , the particle dimension was further reduced, as reflected by the production of Co_3O_4 nanoplatelets with lateral size of 25–30 nm. For the electrochemical performance, excellent stability was observed both in the improved rate capacity of single electrode and the capacitance maintenance of supercapacitor. This study provides a new approach to produce uniformly sized Co_3O_4 nanoparticles for the application in energy storage devices.

Abbreviations

AFM: Atomic force microscopy; BET: Brunauer-Emmett-Teller; CV: Cyclic voltammetry; EIS: Electrochemical impedance spectroscopy; EDS: Energy-dispersive X-ray spectroscopy; FTIR: Fourier transform infrared spectroscopy; GO: Graphene oxide; GCD: Galvanostatic charge/discharge; MWCNTs: Multiwall carbon nanotubes; PVA: Poly(vinyl alcohol); SEM: Scanning electron microscopy; SGP: Sulfonated graphenel polymer; TEM: Transmission electron microscopy; XRD: X-ray diffraction

Acknowledgements

Financial supports from the National Natural Science Foundation of China (11302241, 11404371, 51561145008), Youth Foundation of Natural Science Foundation of Jiangsu Province (BK20140390), Youth Innovation Promotion Association of the Chinese Academy of Sciences (2015256), and National Key Research and Development Program of China (2016YFA0203301) are acknowledged.

Authors' contributions

XHZ prepared the manuscript and supervised all of the study. XZ and XBL performed the experiment. SZ helped in the technical support for the experiments. All the authors discussed the results and approved the final manuscript.

Competing interests

The authors declare that they have no competing interests.

Author details

¹Department of Chemistry, College of Sciences, Shanghai University, Shanghai 200444, China. ²Suzhou Institute of Nano-Tech and Nano-Bionics, Chinese Academy of Sciences, Suzhou 215123, China. ³School of Energy and Power Engineering, University of Shanghai for Science and Technology, Shanghai 200093, China.

Received: 15 November 2016 Accepted: 26 February 2017

Published online: 04 March 2017

References

- Simon P, Gogotsi Y (2008) Materials for electrochemical capacitors. *Nat Mater* 7(11):845–854
- Dunn B, Kamath H, Tarascon JM (2011) Electrical energy storage for the grid: a battery of choices. *Science* 334(6058):928–935
- El-Kady MF, Kaner RB (2013) Scalable fabrication of high-power graphene micro-supercapacitors for flexible and on-chip energy storage. *Nat Commun* 4(2):1475
- Miller JR, Simon P (2008) Electrochemical capacitors for energy management. *Science* 321(5889):651–652

5. Wang H, Liang Y, Mirfakhrai T, Chen Z, Casalongue HS, Dai H (2011) Advanced asymmetrical supercapacitors based on graphene hybrid materials. *Nano Res* 4(8):729–736
6. Zhi M, Xiang C, Li J, Li M, Wu N (2013) Nanostructured carbon-metal oxide composite electrodes for supercapacitors: a review. *Nanoscale* 5(1):72–88
7. Chen H, Zhou S, Wu L (2014) Porous nickel hydroxide-manganese dioxide-reduced graphene oxide ternary hybrid spheres as excellent supercapacitor electrode materials. *ACS Appl Mater Interfaces* 6(11):8621–8630
8. Dong XC, Xu H, Wang XW, Huang YX, Chan-Park MB, Zhang H, et al (2012) 3D graphene-cobalt oxide electrode for high-performance supercapacitor and enzymeless glucose detection. *ACS Nano* 6(4):3206–3213
9. Luan F, Wang G, Ling Y, Lu X, Wang H, Tong Y, et al (2013) High energy density asymmetric supercapacitors with a nickel oxide nanoflake cathode and a 3D reduced graphene oxide anode. *Nanoscale* 5:7984–7990
10. Susanti D, Tsai DS, Huang YS, Korotcov A, Chung WH (2007) Structures and electrochemical capacitive properties of RuO₂ vertical nanorods encased in hydrous RuO₂. *J Phys Chem C* 111(26):9530–9537
11. Garakani MA, Abouali S, Zhang B, Xu ZL, Huang J, Huang JQ, et al (2015) Controlled synthesis of cobalt carbonate/graphene composites with excellent supercapacitive performance and pseudocapacitive characteristics. *J Mater Chem A* 3:17827–17836
12. Wang H, Zhang L, Tan X, Holt CMB, Zahiri B, Olsen BC, et al (2011) Supercapacitive properties of hydrothermally synthesized Co₃O₄ nanostructures. *J Phys Chem C* 115(35):17599–17605
13. Li Y, Zhao N, Shi C, Liu E, He C (2012) Improve the supercapacitive performance of MnO₂-decorated graphene by controlling the oxidation extent of graphene. *J Phys Chem C* 116(48):25226–25232
14. Yang W, Gao Z, Ma J, Wang J, Wang B, Liu L (2013) Effects of solvent on the morphology of nanostructured Co₃O₄ and its application for high-performance supercapacitors. *Electrochim Acta* 112:378–385
15. Kumar R, Kim HJ, Park S, Srivastava A, Oh IK (2014) Graphene-wrapped and cobalt oxide-intercalated hybrid for extremely durable super-capacitor with ultrahigh energy and power densities. *Carbon* 79:192–202
16. Liao Q, Li N, Jin S, Yang G, Wang C (2015) All-solid-state symmetric supercapacitor based on Co₃O₄ nanoparticles on vertically aligned graphene. *ACS Nano* 9(5):5310–5317
17. Guan Q, Cheng J, Wang B, Ni W, Gu G, Li X, et al. (2014) Needle-like Co₃O₄ anchored on the graphene with enhanced electrochemical performance for aqueous supercapacitors. *ACS Appl Mater Interfaces* 6(10):7626–7632
18. Huang ML, Gu CD, Ge X, Wang XL, Tu JP (2014) NiO nanoflakes grown on porous graphene frameworks as advanced electrochemical pseudocapacitor materials. *J Power Sources* 259:98–105
19. Zhao G, Li J, Ren X, Chen C, Wang X (2011) Few-layered graphene oxide nanosheets as superior sorbents for heavy metal ion pollution management. *Environ Sci Technol* 45(24):10454–10462
20. Li X, Song Q, Hao L, Zhi L (2014) Graphene polymers for energy storage. *Small* 10(11):2122–2135
21. Jiang Y, Li J, Hao J Suzhou Graphene-Tech Co., Ltd. Chinese Patent. 201410244717.0
22. Meher SK, Rao GR (2011) Ultralayered Co₃O₄ for high-performance supercapacitor applications. *J Phys Chem C* 115(31):15646–15654
23. Xiang C, Li M, Zhi M, Manivannan A, Wu N (2013) A reduced graphene oxide/Co₃O₄ composite for supercapacitor electrode. *J Power Sources* 226:65–70
24. Liu X, Men C, Zhang X, Li Q (2016) An extraordinary sulfonated-graphene-polymer-based electrolyte separator for all-solid-state supercapacitors. *Small* 12(36):4973–4979
25. Deori K, Deka S (2013) Morphology oriented surfactant dependent CoO and reaction time dependent Co₃O₄ nanocrystals from single synthesis method and their optical and magnetic properties. *CrystEngComm* 15(42):8465–8474
26. Ujjain SK, Singh G, Sharma RK (2015) Co₃O₄@reduced graphene oxide nanoribbon for high performance asymmetric supercapacitor. *Electrochim Acta* 169:276–282
27. Wu ZS, Zhou G, Yin LC, Ren W, Li F, Cheng HM (2012) Graphene/metal oxide composite electrode materials for energy storage. *Nano Energy* 1(1):107–131
28. Sun CY, Zhu YG, Zhu TJ, Xie J, Cao GS, Zhao XB (2013) Co(OH)₂/graphene sheet-on-sheet hybrid as high-performance electrochemical pseudocapacitor electrodes. *J Solid State Electrochem* 17(4):1159–1165
29. Yang Q, Lu Z, Chang Z, Zhu W, Sun J, Liu J, et al (2012) Hierarchical Co₃O₄ nanosheet@nanowire arrays with enhanced pseudocapacitive performance. *RSC Adv* 2:1663–1668
30. Zhu YG, Wang Y, Shi Y, Wong JI, Yang HY (2014) CoO nanoflowers woven by CNT network for high energy density flexible micro-supercapacitor. *Nano Energy* 3:46–54
31. Dong Y, He K, Yin L, Zhang A (2007) A facile route to controlled synthesis of Co₃O₄ nanoparticles and their environmental catalytic properties. *Nanotechnology* 18(43):435602
32. Liang Y, Li Y, Wang H, Zhou J, Wang J, Regier T, et al (2011) Co₃O₄ nanocrystals on graphene as a synergistic catalyst for oxygen reduction reaction. *Nat Mater* 10(10):780–786
33. Feng C, Zhang J, He Y, Zhong C, Hu W, Liu L, et al (2015) Sub-3 nm Co₃O₄ Nanofilms with Enhanced Supercapacitor Properties. *ACS Nano* 9(2):1730–1739
34. Chang MS, Kim T, Kang JH, Park J, Park CR (2015) The effect of surface characteristics of reduced graphene oxide on the performance of a pseudocapacitor. *2D Mater* 2(1):014007
35. Li T, Li S, Zhang B, Wang B, Nie D, Chen Z, et al (2015) Supercapacitor electrode with a homogeneously Co₃O₄-coated multiwalled carbon nanotube for a high capacitance. *Nanoscale Res Lett* 10:208
36. Lu X, Zheng D, Zhai T, Liu Z, Huang Y, Xie S, et al (2011) Facile synthesis of large-area manganese oxide nanorod arrays as a high-performance electrochemical supercapacitor. *Energy Environ Sci* 4:2915–2921

Submit your manuscript to a SpringerOpen[®] journal and benefit from:

- Convenient online submission
- Rigorous peer review
- Immediate publication on acceptance
- Open access: articles freely available online
- High visibility within the field
- Retaining the copyright to your article

Submit your next manuscript at ► springeropen.com